J. Opt. B: Quantum Semiclass. Opt. **2** (2000) 563–569. Printed in the UK PII: S1464-4266(00)07995-7

Carrier dynamics in semiconductor lasers operating in the low-frequency fluctuation regime

M S Torre†, C Masoller‡, N B Abraham§ and H F Ranea-Sandoval†‖

† Instituto de Física 'Arroyo Seco', UNCPBA Pinto 399 (7000) Tandil, Argentina
‡ Instituto de Física, Facultad de Ciencias, Universidad de la República, Montevideo, Uruguay
§ DePauw University, Greencastle, IN 46135-0037, USA

Received 21 September 1999, in final form 24 May 2000

Abstract. We analyse the dynamics of a weakly index-guided semiconductor laser operating near threshold and with optical feedback, using the Lang–Kobayashi model. Lateral effects are included, taking into account lateral carrier diffusion and a lateral profile for the optical field. The laser intensity fluctuates in a sequence of picosecond pulses, and the time-averaged intensity shows sudden dropouts to a nearly zero value, followed by gradual, steplike recoveries. We find that for large carrier diffusion the averaged intensity drops less frequently to zero and recovers less noisily than for low carrier diffusion. We analyse the time evolution of the carriers, and find that at the centre of the active region it fluctuates rapidly following the fast pulsing intensity. Further from the centre of the active region, diffusion has a preponderant effect and the carriers vary more smoothly in time (following the oscillations of the time-averaged intensity). Even further from the centre of the active region, the carrier profile is not influenced by the external optical feedback. The spatial variations of the carrier distribution and of the light intensity distribution within the mode seem to anticipate the occurrence of a dropout.

Keywords: Semiconductor laser, optical feedback, low frequency fluctuation, carrier diffusion

1. Introduction

Low-frequency fluctuations (LFFs) are a well known feedback-induced instability that occurs when a semiconductor laser operates with moderately strong optical feedback from an external cavity. The LFFs consist of sudden intensity dropouts followed by gradual, steplike recoveries (these intensity fluctuations generate a broad feature at low frequencies in the power spectrum, hence they are called LFFs). Streak camera measurements have shown that the LFFs are actually the envelope of a series of fast, picosecond pulses [1–3]. The LFFs were originally studied close to the solitary laser threshold, but they also exist at higher pumping levels [4].

In recent years several investigations of the LFFs have been conducted from the experimental and the theoretical points of view [5–11]. The interest has been centred, in part, in understanding how the dynamics is affected by the multimode behaviour of many of the lasers investigated, and how the competition between different longitudinal modes may influence critically the occurrence of LFFs.

‖ Member of the Carrera del Investigador Científico (CONICET).

Such multimode operation is thought to play a crucial role in the recovery process of the optical power after a dropout. Recent experimental results show that after a dropout, and while the output power is still recovering, many of the longitudinal modes of the solitary laser switch on even though at a later stage, and before the following dropout, the laser operates predominantly in a single longitudinal mode [3, 7, 10, 11].

In spite of the fact that the LFFs are often associated with the excitation of multiple solitary laser modes, numerical simulations of the Lang–Kobayashi (LK) model [12], which assumes single-mode operation, have shown good qualitative agreement with the observations. The model considers the time evolution of the field amplitude coupled to the carrier density, and the effect of the optical feedback is included by means of a time-delayed term that corresponds to a reflection from the external mirror. From the numerical integration of the LK model it has been shown that the time-averaged power exhibits drops similar to those experimentally observed and it was also numerically shown that in a picosecond scale the laser emits pulses [1, 2, 6, 8].

The LFFs predicted by the single-mode LK model were confirmed by the experimental observation of Heil *et al* [8]

1464-4266/00/050563+07$30.00

of LFFs in single-mode distributed-feedback lasers, and by Huyet *et al* [7], in an intrinsically multimode laser that operates in a single mode. (In [7] the laser was biased below the solitary laser threshold and an etalon was placed in the external cavity. The etalon restricts the feedback to just a mode, and since the laser is below threshold, other solitary modes are not excited.)

Since LFFs have been observed in single- and multimode operation, the role of the competition of several longitudinal modes is still not fully understood. Vaschenko and coworkers [3] made spectrally resolved streak camera measurements that show that in multimode operation the modal intensities pulse with arbitrary phases one relative to the other, and that shortly after two or more modes synchronize their amplitudes, to pulse in phase, a drop in the total intensity occurs. Sukow *et al* [2] have shown that the histogram of the intensity fluctuations on a picosecond time scale is essentially independent of the number of modes involved in the laser emission. The statistics obtained from single-mode and multimode configurations were indistinguishable in the experiments and also in the numerical simulations, which were based on the LK model and a multimode extension of the model. In [13] a similar observation is made regarding the multimode operation. These results suggest that although the competition between several longitudinal modes might strongly influence the LFFs, many features of the dynamics in between power dropouts can be successfully modelled by the single-mode LK model.

Carrier diffusion is important to understand the dynamics of semiconductor lasers [14]. Longitudinal carrier diffusion erases the longitudinal grating of the carrier density, strongly affecting the competition between different longitudinal modes of the laser cavity. Lateral carrier diffusion explains that the carrier lifetime obtained from experimental measurements of impedance below threshold is different from that obtained from measurement of spontaneous emission [15]. Rapid lateral carrier diffusion also leads to a strong damping of the relaxation oscillations, which can be observed in the small-signal modulation response [16, 17], and which has important consequences in the dynamics.

In the rate-equation approximation, lateral carrier diffusion is often modelled through a nonlinear gain coefficient. In [2] it was found that multimode operation in the LFF regime does not affect the histogram of the intensity fluctuations, but gain saturation and the coexistence of attractors cause substantial changes, and this effect is more pronounced for pump currents well above threshold. Münkel *et al* [18] studied the LFFs based on a 'transverse LK model' that includes optical diffraction and carrier diffusion. The authors did not investigate the effect of diffusion, but focused on the spatio-temporal feedback-induced instabilities for different laser geometries.

Here, we study the effect of lateral carrier diffusion on the dynamics of a weakly index-guided semiconductor laser operating in the LFF regime. We consider a modification of the LK model that includes lateral carrier diffusion and a lateral profile for the optical field. In the LFF regime, where the intensity is nearly zero between pulses and the average intensity is low, modelling carrier diffusion through a diffusion term might be more accurate than modelling it through a gain saturation coefficient. The difference might be important in the LFFs that occur close to the lasing threshold, where the gain saturation term might not adequately describe the effect of carrier diffusion.

This paper is organized as follows: section 2 describes the theoretical model employed. Section 3 contains the results of the numerical simulations. We show the fluctuations of the instantaneous intensity and the fluctuations of the time-averaged intensity, for different values of carrier diffusion coefficient. In section 4 we study the carrier dynamics during the power dropouts. Section 5 contains our conclusions and a discussion.

2. Theoretical model

The rate equations for an index-guided single-mode semiconductor laser with weak optical feedback, including lateral carrier diffusion and lateral spatial variations of both the optical field and the carrier density, are

$$\frac{\mathrm{d}E(t)}{\mathrm{d}t} = \frac{1+\mathrm{i}\alpha}{2}\left[\frac{\int_{-w/2}^{w/2} F(x)G_N[N(x,t)-N_0]\,\mathrm{d}x}{\int_{-\infty}^{+\infty} F(x)\,\mathrm{d}x} - \frac{1}{\tau_\mathrm{p}}\right] \times E(t) + \gamma E(t-\tau)\exp(\mathrm{i}\omega_0\tau), \quad (1)$$

$$\frac{\partial N(x,t)}{\partial t} = \frac{C(x)}{qd} - \frac{N(x,t)}{\tau_\mathrm{s}} + D\frac{\partial^2 N(x,t)}{\partial x^2} - F(x)G_N[N(x,t)-N_0]|E(t)|^2. \quad (2)$$

Here, $E(t)$ is the complex field amplitude of the fundamental mode with lateral spatial distribution $F(x)$, which is obtained by solving the Helmholtz equation, and $N(x,t)$ is the carrier density. The first term on the right-hand side of (1) accounts for material gain, losses and phase–amplitude coupling, and the second term accounts for weak optical feedback from an external mirror positioned at a distance $L_\mathrm{ext} = c\tau/2$. The speed of the light in vacuum is c and τ is the round-trip time. The feedback strength is γ. The factor $\omega_0\tau$ is called the feedback phase and is the result of the slowly varying amplitude description (ω_0 is the optical frequency without feedback). The right-hand side of (2) accounts for carrier injection, spontaneous recombination, carrier diffusion and stimulated recombination. The parameters are τ_s, the carrier lifetime; τ_p, the photon lifetime; D, the diffusion coefficient; α, the linewidth enhancement factor; $C(x)$, the injected current density; d, the active layer thickness; w, the active layer width, and q, the electron charge. G_N is the differential gain and N_0 is the carrier density at transparency.

Considering the following dimensionless variables:

$$e(t) = E(t)\sqrt{G_N\tau_\mathrm{s}}, \quad (3)$$

$$n(x,t) = \tau_\mathrm{p}G_N[N(x,t)-N_0], \quad (4)$$

equations (1) and (2) can be written as

$$\frac{\mathrm{d}e(t)}{\mathrm{d}t} = \frac{1+\mathrm{i}\alpha}{2}\left[G(t) - \frac{1}{\tau_\mathrm{p}}\right]e(t) + \gamma e(t-\tau)\exp(\mathrm{i}\omega_0\tau), \quad (5)$$

$$\frac{\partial n(x,t)}{\partial t} = \frac{1}{\tau_s}\Bigg[J(x) - n(x,t) + \tau_s D \frac{\partial^2 n(x,t)}{\partial x^2} - n(x,t)F(x)|E(t)|^2 \Bigg], \tag{6}$$

where $G(t)$ is the modal gain given by

$$G(t) = \frac{\int_{-w/2}^{w/2} F(x) n(x,t)\,\mathrm{d}x}{\int_{-\infty}^{\infty} F(x)\,\mathrm{d}x}, \tag{7}$$

and $J(x)$ is the normalized current density given by

$$J(x) = \tau_s \tau_p G_N \left[\frac{C(x)}{qd} - \frac{N_0}{\tau_s} \right]. \tag{8}$$

Since our goal is to study the effect of carrier diffusion in the dynamics, we simplify the model and do not take into account either the diffraction of the light in the external cavity or the spontaneous emission.

3. Results of the numerical simulations

The numerical integration of equations (5) and (6) was performed with a spatial integration step of 0.036 μm and a time integration step of 0.01 ps. We considered uniform injection over the stripe width: $J(x) = j_0$ for $|x| < w/2$ and $J(x) = -\tau_p G_N N_0 = -j_1$ otherwise (since $J(x)$ is the normalized current density, equation (8), $J(x)$ takes the constant negative value $-j_1$ in the region where no carriers are injected). The initial conditions are $n(x,0) = -\tau_p G_N N_0 = -j_1$ for $-\infty < x < +\infty$ (i.e. initially there are no carriers) and $e(t) = 0$ for $-\tau \leqslant t \leqslant 0$. The parameter values used in the simulations are $w = 6$ μm, $\alpha = 4.4$, $\tau_s = 1$ ns, $\tau_p = 1$ ps, $\tau_p G_N N_0 = 0.8$, $\tau = 3$ ns (which corresponds to a external cavity of length 45 cm) and $\omega_0 \tau = 0$ rad.

To study the effect of a lateral distribution of carriers in the dynamics, we consider different values of the diffusion coefficient, D, and different values of the injection current, j_0. Carrier diffusion strongly modifies the threshold current, $j_{0,\mathrm{th}}$, and the effective injected current.

Figure 1 shows the mean output power as a function of the injected current, for three different values of D. A nearly linear relation is found in spite of the large intensity pulsations that occur for this feedback level. For comparison, we show in the dashed curves the output intensity in the three cases in the absence of feedback. For the feedback level considered and $D = 3$ cm^2 s^{-1}, the threshold current density is $j_{0,\mathrm{th}} = 1.02$, while for $D = 60$ cm^2 s^{-1}, $j_{0,\mathrm{th}} = 1.82$. Therefore, the parameter we chose to hold constant for comparison at similar physical situations is the mean output power (and not the percentage above threshold). Hence, for different values of D we consider three different injection currents (for $D = 3$ cm^2 s^{-1}; $j_0 = 1.04, 1.08, 1.14$; and for $D = 60$ cm^2 s^{-1}; $j_0 = 1.84, 1.88, 1.96$) chosen so that the mean output is the same in each case.

Figures 2 and 3 show the time-averaged intensity as a function of time for three different injection currents (we averaged over 1 ns to simulate the bandwidth of the photodetectors commonly used in experiments).

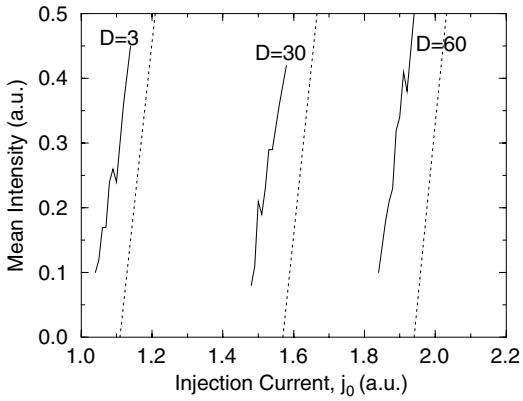

Figure 1. Laser time-averaged intensity as a function of the injected current, for three different values of the diffusion coefficient, D. Dashed curves: no feedback. Solid curves: feedback level of $\gamma = 40$ ns^{-1}.

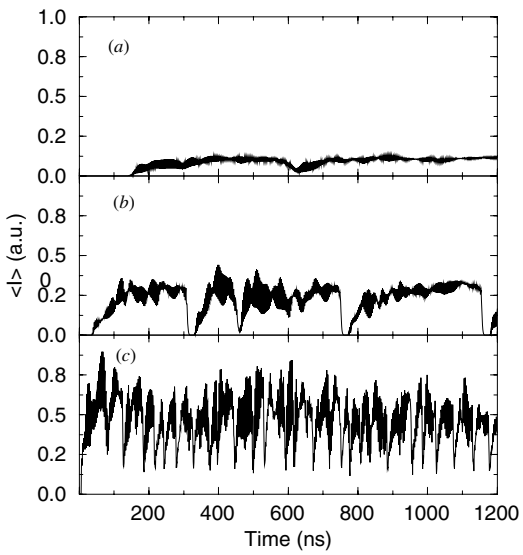

Figure 2. Time-averaged intensity as a function of time for $D = 3$ cm^2 s^{-1} and (*a*) $j_0 = 1.04$, (*b*) 1.08, (*c*) 1.14.

Figure 2 displays the results for the lowest diffusion rate of carriers ($D = 3$ cm^2 s^{-1}, which corresponds to a diffusion characteristic length $L_D = \sqrt{\tau_s D} = 0.5$ μm); and figure 3 for the largest diffusion of carriers ($D = 60$ cm^2 s^{-1}, which corresponds to $L_D = 2.5$ μm). Figures 2(*a*)–(*c*) correspond to figures 3(*a*)–(*c*), with approximately the same (increasing) mean output intensity.

Slightly below the solitary laser threshold there is a long delay in the laser turn-on; the time-averaged intensity shows fluctuations but no clear dropouts and there are no differences between the cases $D = 3$ (figure 2(*a*)) and 60 cm^2 s^{-1} (figure 3(*a*)). For larger injection currents dropouts appear. After a power dropout, the time-averaged intensity does not recover immediately (figures 2(*b*) and 3(*b*)). Above the solitary laser threshold, the delay in the laser turn-on is short, the dropouts are frequent, and after a dropout the time-averaged intensity recovers almost immediately. For even larger injection currents the dropouts become very frequent and cannot be distinguished, and the so-called coherence

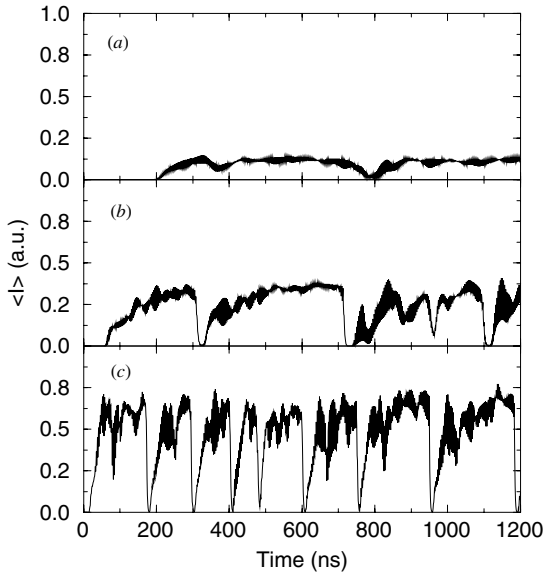

Figure 3. Time-averaged intensity as a function of time for $D = 60$ cm^2 s^{-1} and (*a*) $j_0 = 1.84$, (*b*) 1.88, (*c*) 1.94.

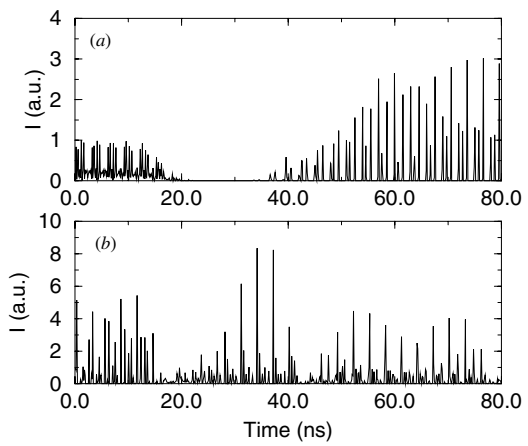

Figure 4. Intensity pulses as a function of time for $\gamma = 40$ ns^{-1}, $D = 3$ cm^2 s^{-1} and (*a*) $j_0 = 1.08$, (*b*) 1.14.

collapsed regime arises.

Comparing figure 2(*c*) with 3(*c*) (which correspond to low and fast carrier diffusion at the same mean output power) we can see that for low carrier diffusion there are larger fluctuations of the averaged intensity and more frequent and shorter dropouts and the signal is noisier. To understand these results we study the fluctuations of the instantaneous intensity and the dynamics of the carriers during the dropouts.

Figures 4(*a*), (*b*) and 5(*a*), (*b*) display, for the same parameter values as for figures 2(*b*), (*c*) and 3(*b*), (*c*) respectively, the instantaneous intensity as a function of time during a power dropout. The dropouts differ depending on the injection current. Slightly above the solitary laser threshold (figures 4(*a*) and 5(*a*)), before the power dropout, the intensity shows relatively small fluctuations around a mean value that differs from zero. After the dropout there is a delay (of about 20 ns), and then the intensity recovers in trains of pulses, which have a marked pseudoperiodicity at the external cavity round trip time.

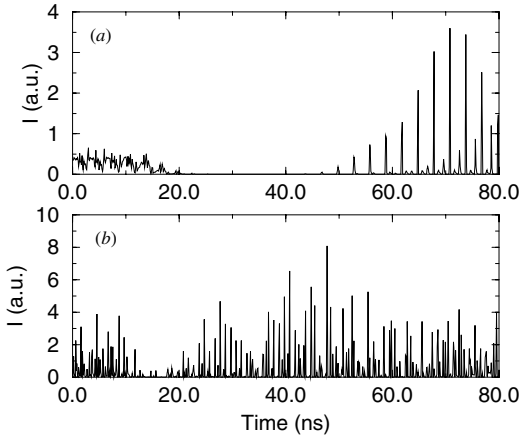

Figure 5. Intensity pulses as a function of time for $\gamma = 40$ ns^{-1}, $D = 60$ cm^2 s^{-1} and (*a*) $j_0 = 1.88$, (*b*) 1.94.

During a first stage (that takes about five round trips) these pulses increase nearly exponentially in time (this can be seen in a logarithmic plot, not shown). For a low value of the carrier diffusion rate, figure 4(*a*), the relaxation oscillations that appear are practically undamped; in contrast, for a large value of the carrier diffusion rate, figure 5(*a*), the relaxation oscillations are strongly damped. In the latter case, the arrival of the feedback pulse occurs when the system has already reached the steady state; in the former case (for lower D), the arrival occurs when the system is still oscillating. In other words, there is a pulsing with a repetition rate controlled by the external cavity round-trip time, and pulsing also exists at shorter timescales, which is the influence of the high relaxation–oscillation frequency. It is worth mentioning that similar results were experimentally observed in [3] for the behaviour of the total intensity, in a multimode laser in the LFF regime. The effect of diffusion is, as would be intuitively expected, a consequence of the damping of the relaxation oscillations. The higher frequencies observed at lower D values will produce a time average intensity diagram (figure 2) richer in higher frequencies, which give the trace a much noisier appearance. This might explain why the average intensity is noisier in the first case than in the other.

For larger values of the injection current (figures 4(*b*) and 5(*b*)), there are strong intensity pulsations (departing from zero) before and after the power dropout.

To investigate the effect of carrier diffusion in the statistics of the intensity fluctuations, we calculated the histogram of the intensity pulses underlying the dropouts of the average intensity. We studied the time series corresponding to the average intensity shown in figures 2 and 3; the first 400 ns were not considered in the histograms to avoid transient effects. Figure 6 shows the results obtained. For easy comparison with previously reported results, the data are plotted in a vertical logarithmic scale. We find that for slow and fast carrier diffusion the histograms are similar for the three injection currents considered, and they resemble the experimentally and numerically obtained histograms reported in [2, 7]. For low injection current the histograms are double peaked: they have a peak at zero-intensity and at a non-zero intensity value. As j_0 increases, the non-zero intensity peak diminishes until it disappears.

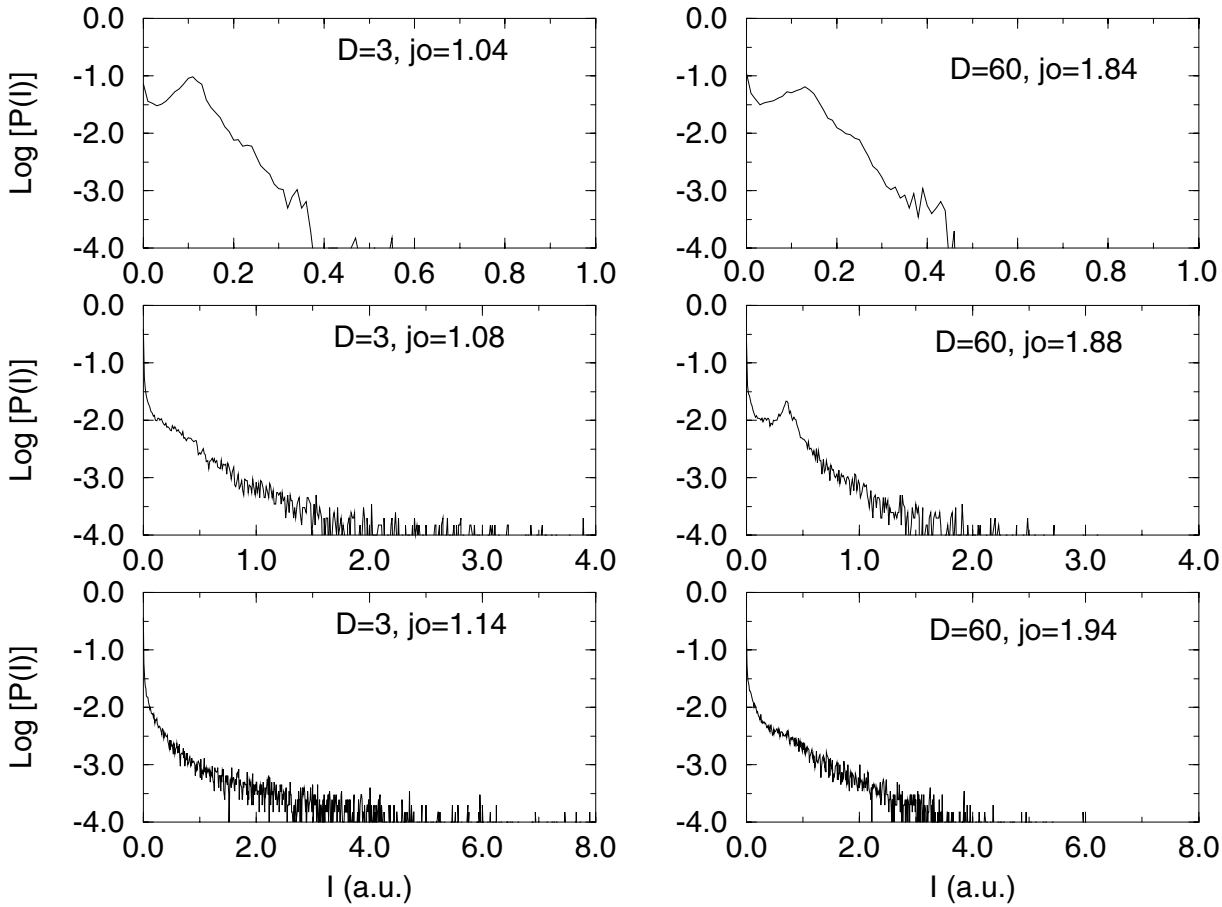

Figure 6. Histogram of the intensity of the pulses for $D = 3$ cm^2 s^{-1} and $j_0 = 1.04, 1.08, 1.14$; and $D = 60$ cm^2 s^{-1} and $j_0 = 1.84, 1.88, 1.94$. The intensity fluctuations correspond to the fast dynamics underlying the average evolution shown in figures 3 and 4. The first 200 ns are not considered in the histogram, to avoid transient effects.

For $D = 3$ cm^2 s^{-1}, $j_0 = 1.08$ this peak is lower and wider than for $D = 60$ cm^2 s^{-1}, $j_0 = 1.88$. For larger injection currents the probability of low intensity values is larger for $D = 3$ cm^2 s^{-1} than for $D = 60$ cm^2 s^{-1} (this can be appreciated plotting the probability $P(I)$ in a linear vertical scale, not show here). These results indicate that, for injection currents above the solitary threshold, the laser remains longer in the steady state for fast carrier diffusion than for low carrier diffusion. Although for fast and slow carrier diffusion the histograms of the intensity fluctuations are similar besides the above-mentioned features, we will show in the next section that the underlying laterally resolved carrier dynamics is very different in the two cases.

4. Carrier dynamics

The fast intensity pulses lead to fast time variations in the carrier profile. Figure 7 shows the instantaneous carrier density profile $n(x, t)$ (for $D = 3$ cm^2 s^{-1} solid curve, for $D = 60$ cm^2 s^{-1} dashed curve) at the final time $t \approx 80$ ns (the dotted curve shows the optical mode profile for comparison). The variable $n(x, t)$ represents the difference between the actual carrier density and the carrier density at transparency, equation (4); therefore, negative values of $n(x, t)$ indicate that

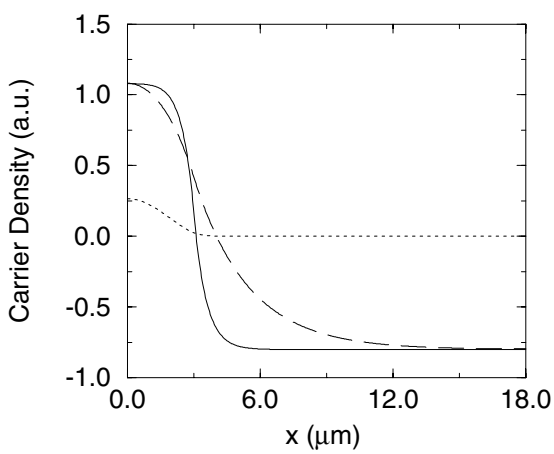

Figure 7. Carrier density profile for $\gamma = 40$ ns^{-1}, $D = 3$ cm^2 s^{-1} and $j_0 = 1.14$ (solid curve), and $D = 60$ cm^2 s^{-1} and $j_0 = 1.94$ (dashed curve). For comparison we plot the lateral optical mode profile, $F(x)$ (dotted curve).

the actual carrier density is lower than the transparency value. Lateral spatial hole burning is observed for $D = 3$ cm^2 s^{-1}, while the rapid diffusion of carriers for $D = 60$ cm^2 s^{-1} eliminates the hole burning. This result is due to the fact that

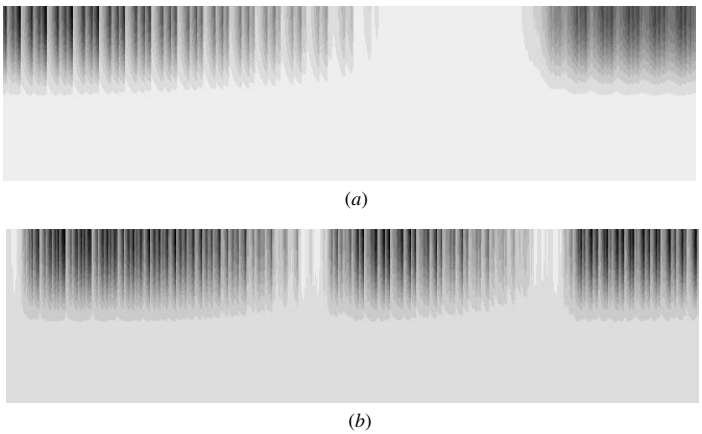

(*a*)

(*b*)

Figure 8. Carrier spatio-temporal dynamics for $\gamma = 40\ \mathrm{ns}^{-1}$, $D = 3\ \mathrm{cm}^2\ \mathrm{s}^{-1}$ and (*a*) $j_0 = 1.08$, (*b*) 1.14. The carrier fluctuations correspond to the intensity pulses shown in figures 4(*a*) and (*b*) respectively. The difference $n(x, t) - n_{\gamma=0}(x)$, where $n_{\gamma=0}(x)$ is the stationary carrier density profile in the absence of feedback, is represented in a scale of 15 grey tones: the darker (lighter) one represents the most negative (positive) value.

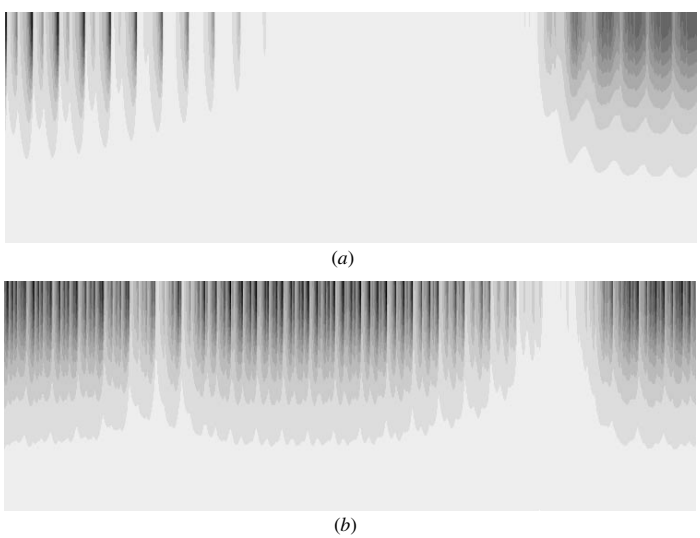

(*a*)

(*b*)

Figure 9. As figure 8 but for $\gamma = 40\ \mathrm{ns}^{-1}$, $D = 60\ \mathrm{cm}^2\ \mathrm{s}^{-1}$ and (*a*) $j_0 = 1.88$, (*b*) 1.94. The carrier fluctuations correspond to the intensity pulses shown in figures 5(*a*) and (*b*) respectively.

the only mechanism to smooth out the non-uniform carrier depletion in the active layer is the carrier diffusion.

We illustrate the time variations of the carrier profile in spacetime representations in figures 8 and 9 (figures 8(*a*), (*b*); 9(*a*), (*b*) correspond to the intensity fluctuations shown in figures 4(*a*), (*b*); 5(*a*), (*b*), respectively). In all figures, the x-axis runs from $x = 0$ to w. The carriers are injected in the region $x = 0$–$w/2$, where the optical mode is different from zero. The time axis runs from $t = 0$ to $t \approx 80$ ns and increases downwards. The value of the difference $n(x, t) - n_{\gamma=0}(x)$, where $n_{\gamma=0}(x)$ is the stationary carrier density profile in the absence of feedback, is represented in grey tones.

Since the fluctuations of the carrier density, $\delta n(x, t)$, are much smaller than the actual value of the carrier density, $n(x, t)$, to clearly see the magnitude of the fluctuations of the carrier profile (in a scale of 15 grey tones) we subtract $n_{\gamma=0}(x)$ from $n(x, t)$ ($n_{\gamma=0}(x)$ is a carrier profile constant in time). Therefore, in the diagrams, the darker tones represent zones where the carrier density is lower than the carrier density in the absence of feedback.

Figure 8(*a*) corresponds to the intensity fluctuations shown in figure 4(*a*), in which there is low injection current and low diffusion of carriers. The carrier profile outside the active region is almost the profile without feedback, while the dark zones in the interval $x < w/2$, indicate that in this region the carrier profile is lower than $n_{\gamma=0}(x)$. Since the diffusion coefficient is low, the carriers that are outside the active region do not respond to the pulsing optical field fast enough.

In contrast, in the case of fast carrier diffusion (figure 9(*a*)), which corresponds to the intensity fluctuations shown in figure 5(*a*), the carriers outside the active region are affected by the fast intensity fluctuations.

The intensity pulses deplete the carriers inside the active region and the large value of D allows the carriers outside the active region to move towards the centre and fill the holes. However, this process is slower in time compared with the fast pulses, and therefore the carrier density outside the active region appear to follow the average intensity.

The large white region in the diagrams of figures 8(*a*) and 9(*a*) correspond to the time intervals when a dropout occurs. While the intensity is nearly zero the carrier population grows. Following this region there are dark fringes that are patterns of grey tones that appear periodically in time (each round-trip time). As time evolves, the trains of grey patterns occupy progressively larger space regions. There are different patterns for different D. In the case of a large value of D($D = 60$ cm^2 s^{-1}), there is a dark zone followed by a grey one (larger) and a lighter one (even larger). Our physical interpretation is that the dark zone corresponds to the time during which there is a light pulse travelling through the active medium; the grey and lighter zones that follow correspond to a replenishment of the carriers that were depleted by the optical pulse. The smaller characteristic time of the large diffusion rate in the case $D = 60$ cm^2 s^{-1} allows the replenishment to be completed before the next pulse arrives (therefore allowing a lighter grey zone). For smaller D ($D = 3$ cm^2 s^{-1}) the slow characteristic time of the diffusion does not allow the replenishment to finish before the next pulse arrives, and therefore there are not as many light-grey zones in figure 9(*a*). The effect of the diffusion is more evident for low carrier injection rates, and is washed out by the external feedback in the case of more rapid injection rates (figures 8(*b*) and 9(*b*)). For larger injection current, the dropouts are shorter in time since the large injection rates do not allow gain to remain depressed as long and thus the intensity does not drop to zero for as long a time.

5. Conclusions and discussions

We have studied a modification of the single-mode LK equations that includes carrier diffusion and lateral profiles for the carriers and the optical mode. We find dropouts in the output intensity for low and high values of the carrier diffusion coefficient. Diffusion appears to modify the dynamic of the intensity (in average and in instantaneous fluctuations). The main effect of carrier diffusion is to modify the dynamics of relaxation oscillations. For low carrier diffusion, relaxation oscillations are weakly damped and the intermingling of intensity oscillations with the pulses returning from the external cavity introduces a great complexity in the signal, appearing to be noise. By contrast, at higher D values the relaxation oscillations are strongly damped, which makes the signal look clearer.

The dynamics of the carriers during the dropouts was studied in detail, and we find that it depends strongly on the value of the diffusion coefficient. The role played by carrier diffusion was illustrated conveniently by space–temporal plots, where the value of the carrier density is represented in grey tones. We can explain the different patterns through the non-uniformity of the carrier profile. We find that the carrier density at the centre of the active region fluctuates rapidly, following the fast intensity fluctuations. Further from the centre of the active region the carriers vary smoothly in time (following the oscillations of the average intensity). Even further from the centre of the active region the carrier profile is almost constant in time and is the profile of the carriers without feedback. In the case of fast carrier diffusion the carriers outside the active region are affected by the fast intensity fluctuations. The intensity pulses deplete the carriers inside the active region and the large value of D allows the carriers outside the active region to move towards the centre and fill the holes. However, this process is slower in time than the fast pulsing rates, and therefore the carrier density outside the active region follows the average intensity.

Our results suggest that diffusion effects are important for an understanding of the phenomenon of LFFs. This might be a mechanism that enhances the lateral mode competition for the carrier providing the optical gain. It would be interesting in future studies to investigate the effect of the competition of various lateral modes, and the effect of asymmetric feedback (focusing the field in a particular region of the active medium).

Acknowledgments

This work was partially supported by grants of Agencia Nacional de Promoción Científica y Tecnológica, PMT-PICT 0104, of UNCPBA and of Comisión Sectorial de Investigación Científica (CSIC-URUGUAY).

References

[1] Fischer I, van Tartwijk G H M, Levine A M, Elsäßer W, Göbel E and Lenstra D 1996 *Phys. Rev. Lett.* **76** 220
[2] Sukow D W, Heil T, Fischer I, Gavrielides A, Hohl-AbiChedid A and Elsäßer W 1999 *Phys. Rev.* A **60** 667
[3] Vaschenko G, Giudici M, Rocca J J, Menoni C S, Tredicce J R and Balle S 1998 *Phys. Rev. Lett.* **81** 5536
[4] Pan M-W, Shi B-P and Gray G R 1998 *Opt. Lett.* **22** 166
[5] Takiguchi Y, Liu Y and Ohtsubo J 1998 *Opt. Lett.* **23** 1369
[6] Heil T, Fischer I and Elsäßer W 1999 *Phys. Rev.* A **60** 634
[7] Huyet G, White J K, Kent A J, Hegarty S P, Moloney J V and McInerney J G 1999 *Phys. Rev.* A **60** 1534
[8] Heil T, Fischer I, Elsäßer W, Mulet J and Mirasso C R 1999 *Opt. Lett.* **24** 275
[9] Gavrielides A, Newell T C, Kovanis V, Harrison R G, Swanston N, Yu D and Lu W 1999 *Phys. Rev.* A **60** 1577
[10] Huyet G, Hegarty S P, Giudici M, De Bruyn B and McInerney J G 1997 *Europhys. Lett.* **40** 619
[11] Huyet G, Balle S, Giudici M, Green C, Giacomelli G and Tredicce J R 1998 *Opt. Commun.* **149** 341
[12] Lang R and Kobayashi K 1980 *IEEE J. Quantum Electron.* **16** 347
[13] Mulet J and Mirasso C 1999 *Phys. Rev.* E **59** 5400
[14] Agrawal G P and Dutta N K 1993 *Semiconductor Lasers* (New York: Van Nostrand–Reinhold)
[15] Torre M S, Esquivias I, Romero B, Czotscher K, Weisser S, Ralston J D, Larkins E, Benz W and Rosenzweig J 1997 *J. Appl. Phys.* **81** 6268
[16] Tucker R S and Pope D J 1983 *IEEE J. Quantum Electron.* **19** 1179
[17] Torre M S and Esquivias I 1999 *SPIE Proc.* **3572** 422
[18] Münkel M, Kaiser F and Hess O 1998 *Int. J. Bif. Chaos* **8** 951